Bioconjugate Chemistry

Communication

Multifunctional tumor-targeting cathepsin B-sensitive gemcitabine prodrug covalently targets albumin in situ and improves cancer therapy

Huicong Zhang, Zhisu Sun, Kuanglei Wang, Na Li, Hongxiang Chen, Xiao Tan, Lingxiao Li, Zhonggui He, and Jin Sun

Bioconjugate Chem., **Just Accepted Manuscript** • DOI: 10.1021/acs.bioconjchem.8b00223 • Publication Date (Web): 18 May 2018

ACS Publications is published by the American Chemical Society. 1155 Sixteenth Street N.W., Washington, DC 20036

GAMOriginal Research Communication

Title:

Multifunctional Tumor-Targeting Cathepsin B-Sensitive Gemcitabine Prodrug Covalently Targets Albumin In Situ and Improves Cancer Therapy

Authors: Huicong Zhang[a], Zhisu Sun[a], Kuanglei Wang[b,c], Na Li[d], Hongxiang Chen[e], Xiao Tan[f], Lingxiao Li[g,h], Zhonggui He[a,*], Jin Sun[a,*]

Affiliations:

[a]Department of Pharmaceutics, Wuya College of Innovation, Shenyang Pharmaceutical University, Shenyang, Liaoning, 110016, P. R. China

[b]Wuyi University, Jiangmen, Guangdong, 529020, P. R. China

[c]International Healthcare Innovation Institute (Jiangmen), Jiangmen, Guangdong, 529080, P. R. China

[d]Clinical Pharmacy, Wuya College of Innovation, Shenyang Pharmaceutical University, Shenyang, Liaoning, 110016, P. R. China

[e]Center for Drug Evaluation, China Food and Drug Administration, Beijing, 100022, P. R. China

[f]School of Pharmacy, Shenyang Pharmaceutical University, Shenyang, Liaoning, 110016, P. R. China

[g]School of Pharmacy, Queen's University of Belfast, 97 Lisburn Road, Belfast BT9 7BL, Northern Ireland, UK

[h]School of Pharmacy, China Medical University, Shenyang, Liaoning, 110013, P. R. China

***Corresponding author:**

Prof. Zhonggui He, Ph.D and Prof. Jin Sun, Ph.D

No. 59 Mailbox, Department of Pharmaceutics, Wuya College of Innovation, Shenyang Pharmaceutical University, NO. 103 Wenhua Road, Shenyang 110016, China

Tel: +86-024-23986321; Fax: +86-024-23986321

E-mail address: hezhonggui@vip.163.com; sunjin@syphu.edu.cn

ABSTRACT

We report a new type of amide bond-bearing cathepsin B-sensitive gemcitabine (GEM) prodrugs, capable of *in situ* covalently targeting circulating albumin and then making a hitchhike to the tumor. Specially, less plasma-enzyme deactivation, long plasma half-life, independence on nucleoside transporters, outstanding tumor targeting and site-specific drug release are achieved and such these multifunctional advantages contribute to the dramatically increased *in vivo*

antitumor efficacy.

Key words: Gemcitabine prodrug, Circulating albumin, Hitchhike, Tumor targeting, Cathepsin B-sensitive.

Many factors limit the clinical use of GEM: (a) very short plasma half-life resulting from rapid deamination into inactive 2′-deoxy-2′, 2′-difluorouridine (dFdU) by ubiquitous cytidine deaminase (CDA) in the bloodstream[1-2]; (b) acquired drug resistance (ADR) caused by reduced expression of nucleoside transporters, especially human equilibrative nucleoside transporter (hENT) required for GEM uptake by cancer cells[3-4]; (c) lack of tumor-specific delivery. Up until now, there have been two major solutions to address the above problems, nanoparticulate delivery systems and lipophilic gemcitabine prodrugs[5-6], but the two strategies have only succeeded in one or two aspects aforementioned. Therefore a novel method to win in all aspects and to show great potential towards clinical translation is still in an urgent need[5, 7]. *In vivo* macromolecular prodrug strategy may serve as a promising alternative[8-9]. The strategy applied here employs rapid covalently binding of endogenous circulating albumin with maleimide-containing prodrugs. INNO-206 is a successful example[10-11].

With approximately 19 days plasma half-life and excellent accumulation capacity in solid tumors, albumin becomes an ideal drug carrier for chemotherapeutic drugs[12-13]. *In vivo* albumin-binding prodrugs would have several advantages: (a) enhanced stability against enzyme deactivation in systemic circulation; (b) prolonged retention time in the bloodstream; (c) possible change in cell entry pathway to circumvent special transporters required for hydrophilic drugs; (d) tumor-specific drug delivery; (e) avoiding the use of exogenous albumin which may be expensive and even immunogenic or pathogenic; (f) cheap and simple manufacture as well as quality control, just like other small-molecule drugs.

To achieve site-specific drug release, the enzyme-based approach represents an elegant biocompatible method of both high sensitivity and selectivity[19], when compared with other delivery approaches utilizing certain internal or external stimuli, such as pH, temperature, and light. Cathepsin B is exactly a lysosomal cysteine proteinase only overexpressed in tumors and has therefore been an ideal target for enzyme-triggered, tumor-targeting delivery[14-16]. Moreover, albumin-prodrug conjugates allow for the albumin-mediated cellular entry into cells in a hENTindependent manner of GEM, leading to circumvention of corresponding ADR. So we incorporate a cathepsin B-sensitive linker into the GEM prodrug to obtain hyper-selective tumor bioactivation, lower off-target toxicity and even bypass ADR.

Herein, we synthesized a novel prodrug (GAM) of GEM, equipping GEM with maleimide group through an amide bond-bearing cathepsin B-sensitive linker (**Figure 1)**. Another similar prodrug (GCM) with a carbamate bond-bearing non-cathepsin B-sensitive linker was used as a control (**Figure 2B**).

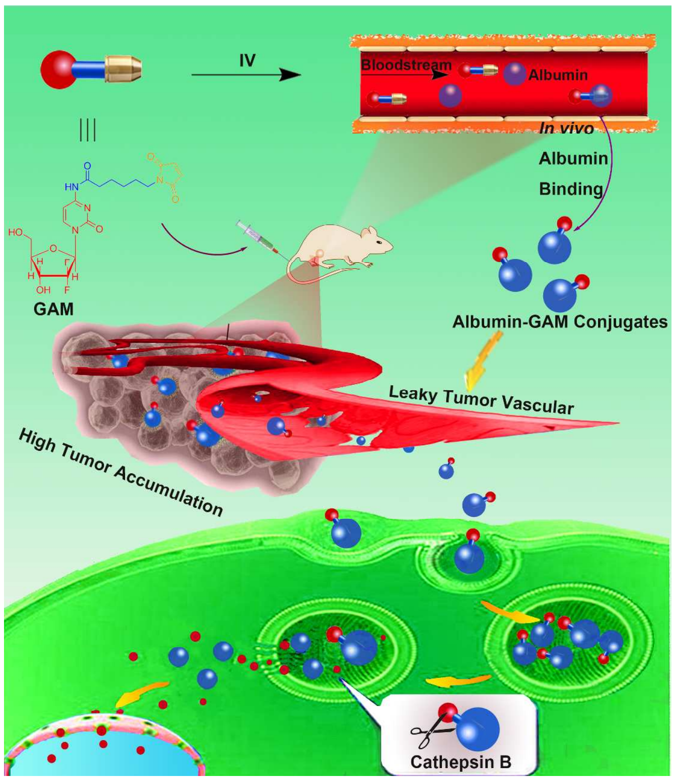

Figure 1. Schematic diagram to describe the whole process of GAM covalently targeting albumin *in situ*, accumulating at the tumor target and then cathepsin B-mediated parent drug release after intravenous administration.

First, GAM was synthesized according to the synthetic routes shown in **Figure 2A**. Maleic anhydride (**3**) and 6-aminocaproic acid were refluxed in glacial acetic acid to obtain 6-maleimidocaproic acid (**4**, **EMC**). The two hydroxyl groups of GEM were masked by TBS groups to furnish compound **2**. Then compounds **2** and **4** were reacted in the presence of HATU to afford **5**. Finally, tetrabutylammonium fluoride (TBAF) unveiled the protective groups of **5** to give target compound GAM. The identity of GAM was confirmed by ^{1}H NMR (**Figure S1**) and MS.

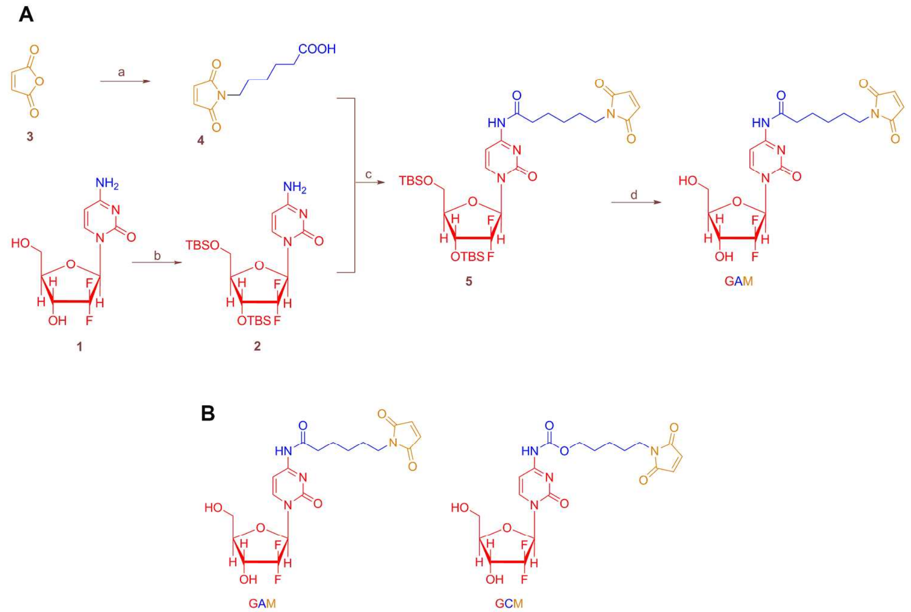

Figure 2. (A) Synthesis of GAM[a]. (B) structures of GAM and GCM.

[a]Reagents and Reactants: (a) 6-aminocaproic acid, glacial acetic acid. (b) TBSCl, imidazole, dichloromethane. (c) HATU, 4-Methylmorpholine, dichloromethane. (d) TBAF, THF.

To investigate the binding ability of GAM with albumin, an *in vitro* binding test was carried out using an HPLC method and the binding ability was measured by the decrease in the prodrug peak intensity. As shown in **Figure 3A,** the majority (ca. 90%) of GAM came into conjugation with BSA within the first 1 min and the binding process almost completed after 30 min incubation. However, when free Cys-34 of BSA was blocked by excessive 6-maleimidocaproic acid (EMC) added in advance, the peak of GAM showed only marginal decrease. The above result validated the specificity of GAM conjugation with albumin through the -SH group of Cys-34.

Another binding test, by *in vitro* incubation with fresh rat blood, came to the same conclusion. Nearly all GAM disappeared after incubation for 1 min (**Figure 3B**), demonstrating a quick albumin-binding rate in blood. By contrast, GAM exhibited no obvious change after incubation for 1 min with blood preincubated with excessive EMC.

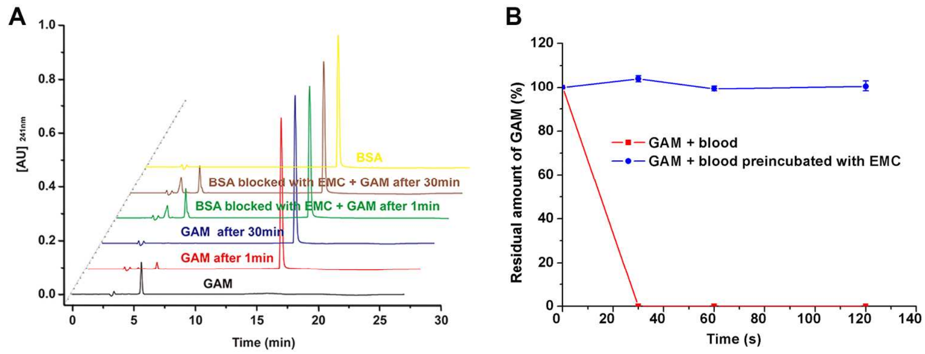

Figure 3. The binding abilities of GAM with albumin at 37°C. (A) Chromatograms. (B) Incubation study of GAM with fresh rat blood (n=3).

GAM existed mainly in the form of albumin-GAM conjugates after intravenous administration, so we prepared BSA-GAM in advance to investigate the enzyme-sensitivity of GAM *in vitro*. Experiments were conducted under different pH values with or without cathepsin B. At pH 7.4, less than 3% of GEM was released from BSA-GAM within 72 h (**Figure 4**), illustrating that the albumin-GAM conjugates could retain good stability under physiological conditions (i.e., in the blood circulation). In contrast, the BSA-GAM showed dramatically accelerated GEM release in the presence of cathepsin B at pH 5.4 (simulated conditions in endosomes and lysosomes) due to the degradation of the amide bond-bearing linker between GEM and albumin. However, the non-enzyme sensitive control, BSA-GCM, released less GEM either in the presence or absence of cathepsin B at corresponding pH.

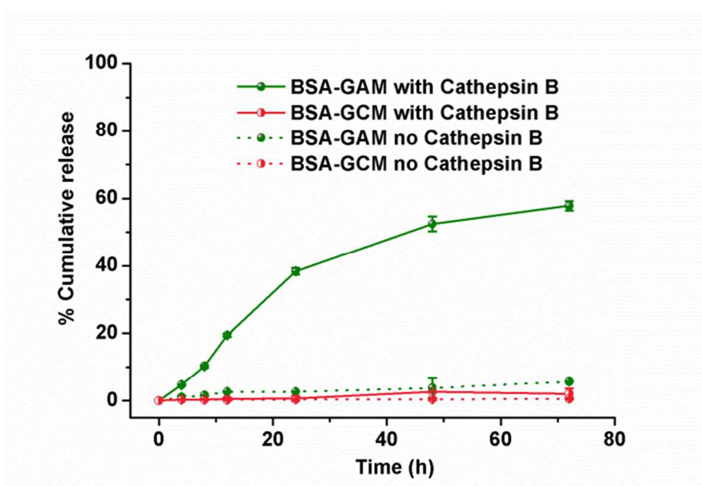

Figure 4. Release of GEM from BSA-GCM and BSA-GAM with cathepsin B at pH 5.4 or without cathepsin B at pH 7.4 (n=3).

To test the stability of BSA-GAM conjugates against metabolism by CDA, GEM, BSA-GAM and BSA-GCM were incubated with fresh rat plasma at an equivalent GEM concentration of 16 μg/mL at 37°C for 12 h, respectively. Both the free GEM and the degraded dFdU product were detected. GEM release rate in the plasma for BSA-GAM and BSA-GCM was comparable to that in buffer at pH 7.4. As shown in **Figure 5A**, no more than 5% of free GEM was released from either BSA-GAM or BSA-GCM group. In **Figure 5B**, the area under the curve (AUC) of the dFdU from BSA-GAM group (AUC: 160 ng·mL^{-1}·h) was 17.5 times lower than that from the GEM group (AUC: 2960 ng·mL^{-1}·h). These data suggested that CDA-dependent degradation only occurred in the free form of GEM and the albumin-conjugated form could provide a good shielding effect from albumin.

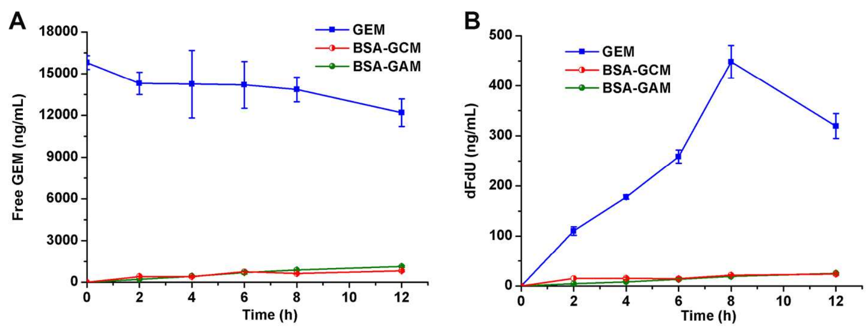

Figure 5. Metabolic stability of GEM and two BSA-prodrug conjugates against CDA in fresh rat blood. (A) Concentration change of free GEM. (B) Concentration change of dFdU (n=3).

Next, Cy5-labelled BSA-GAM conjugates were synthesized to investigate the cellular uptake[17-18]. BSA-GAM and Cy5-BSA-GAM showed similar circular dichroism (CD) spectra to that of BSA (**Figure 6A**), implying that the synthesis process had a negligible influence on the secondary structure of BSA. 4T1 tumor cells were incubated with Cy5-BSA, Cy5-BSA-GAM and Cy5-BSA-GCM for different time and temperature. As shown in **Figure 6B**, cellular uptake of BSA, BSA-GCM and BSA-GAM depended on both time and temperature and demonstrated no significant difference quantitatively. It suggested that small-molecule bioconjugation did not affect the albumin cellular uptake performance.

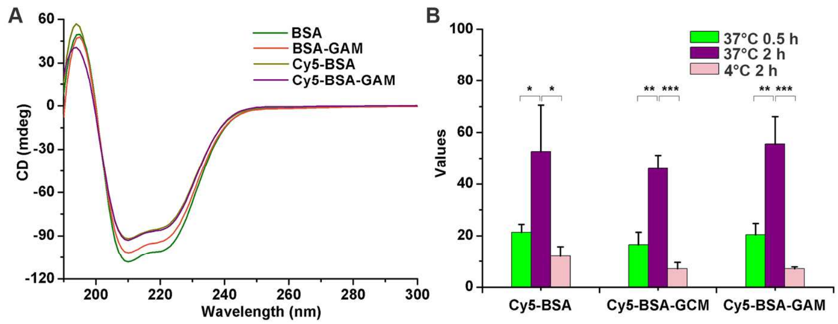

Figure 6. (A) CD spectra of BSA, BSA-GAM, Cy5-BSA and Cy5-BSA-GAM. (B) Cellular uptake of Cy5-BSA, Cy5-BSA-GCM, Cy5-BSA-GAM after incubation with cells at 37°C for 0.5 or 2 h, or at 4°C for 2 h, $^*P < 0.05$, $^{**}P < 0.01$, $^{***}P < 0.001$ (n=3).

To determine whether GEM could be released from albumin-GAM conjugates after cellular uptake, BSA-GAM and BSA-GCM were incubated with 4T1 tumor cells for 6, 12 and 18 h. BSA-GAM demonstrated significantly accelerated intracellular GEM release when compared with the non-stimuli-sensitive control BSA-GCM (**Figure 7**).

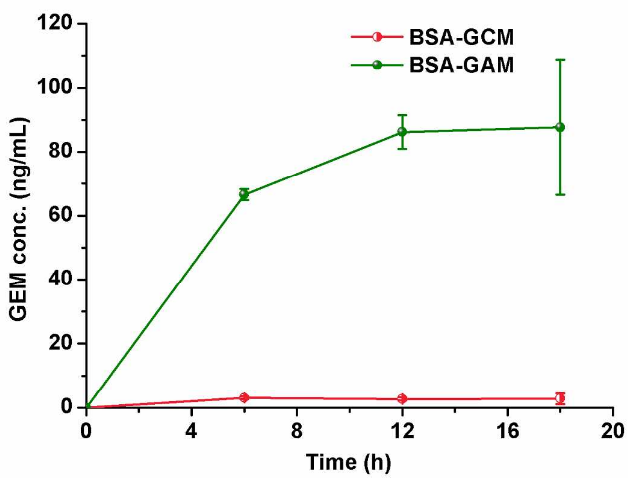

Figure 7. Intracellular GEM release from BSA-GAM and BSA-GCM inside 4T1 cells (n=3).

The cytotoxicity results (**Table S1**) were in a good agreement with the intracellular GEM release experiments. GEM was a potent growth inhibitor for 4T1 cells with IC_{50} value being 9.7 ± 1.2 nM. However, given the delayed release of GEM, both free GAM and BSA-GAM demonstrated less cytotoxicity but still exhibited IC_{50} values in the low micromolar range (0.2-0.5 μM). In contrast, both free GCM and BSA-GCM showed very poor cytotoxicity. Additionally, cytotoxicity of different prodrugs against A549 cells was listed in **Table S2**.

In order to investigate the sensitivity of nucleoside transporter-dependent membrane permeation of BSA-GAM, dipyridamole (DP) was used as an inhibitor of hENT during cytotoxicity evaluation (**Table S1**). In 4T1 cells, DP significantly undermined GEM cytotoxicity by 34 times, while didn't affect the cytotoxicity of BSA-GAM. The results suggested that BSA-GAM entered into tumor cells in a nucleoside transporter-independent but albumin receptor-dependent manner, probably circumventing ADR mediated by decreased expression of hENT.

Pharmacokinetic profile was studied in male Sprague-Dawley (SD) rats. GEM, GCM and GAM were intravenously administrated at an equivalent GEM dose of 1 mg/kg. As shown in **Figure 8A** and **Table S3**, the AUC of free GEM from the GA

M group was less than the half of the GEM group, while $t_{1/2}$ value of free GEM from the GAM group was 5.5 times longer than that of the GEM group. Moreover, the dFdU generated by the GEM group was 6.6 times higher than that of the GAM group (**Figure 8B**). The above data suggested the role of albumin-GAM as a GEM reservoir and protector, leading to less free GEM exposure to plasma-rich CDA.

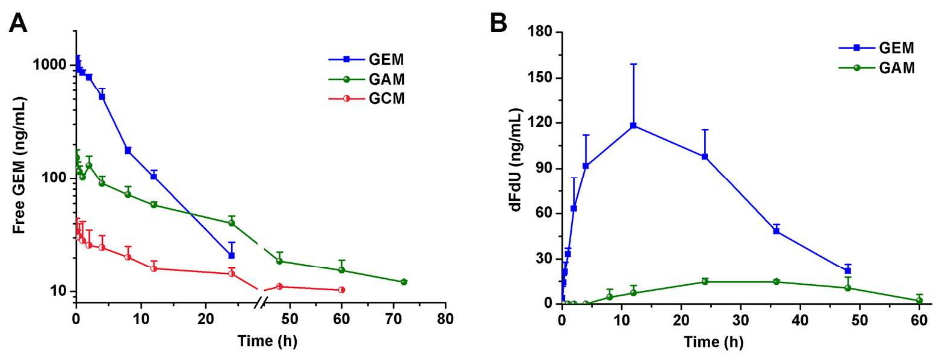

Figure 8. Pharmacokinetic profiles of GEM, GAM and GCM in SD rats. (A) Plasma concentration–time curves of free GEM. (B) Plasma concentration–time curves of dFdU (n=4).

The *in vivo* and *ex vivo* distribution of albumin and albumin-prodrug conjugates was studied in mice bearing 4T1 tumor. Free Cy5 was eliminated quickly from the body and did not manifest obvious accumulation in special organs, while Cy5-BSA, Cy5-BSA-GAM and Cy5-BSA-GCM showed strongest fluorescence of tumor sites either in *in vivo* imaging (**Figure 9A**) or among the dissected organs (**Figure 9C**). Surprisingly, both BSA and BSA-prodrug conjugates could bypass renal elimination and mononuclear phagocytic system deeply plaguing nanoparticulate drug delivery systems, which was validated by the weaker fluorescence intensity of the liver, spleen and kidney than that of the tumor. These data highlighted the outstanding performance of albumin-prodrug conjugates in tumor targeting and sparing much less distribution in normal tissues and organs.

Encouraged by these results, we determined tumor free-GEM accumulation in 4T1 tumor-bearing mice. As shown in **Figure 10A** and **10B**, the tumor free-GEM accumulation of the GAM group was 2.6 times greater than that of GEM solution group. However, GCM showed poor tumor free-GEM accumulation which was even a little less than that of GEM. It was speculated that lack of an enzyme-sensitive linker significantly hindered the release of free GEM from albumin-GCM conjugates and directly limited the accumulation of free GEM in the tumor.

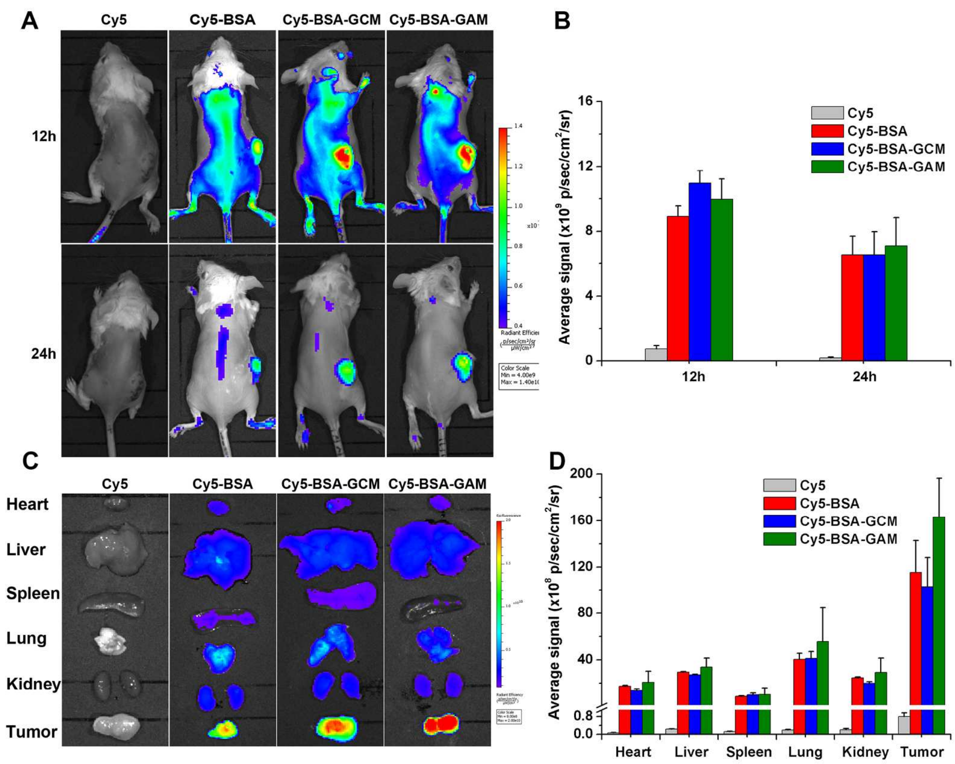

Figure 9. The *in vivo* and *ex vivo* fluorescence imaging of 4T1 tumor-bearing mice after intravenously injection of Cy5, Cy5-BSA, Cy5-BSA-GAM and Cy5-BSA-GCM. (A) Whole-body distribution for 12 and 24 h. (B) Quantitative analysis of relative tumor accumulation in a live body. (C) Relative dissected major organs harvested at 24 h post-administration. (D) Quantitative analysis of relative dissected major organs (n=3).

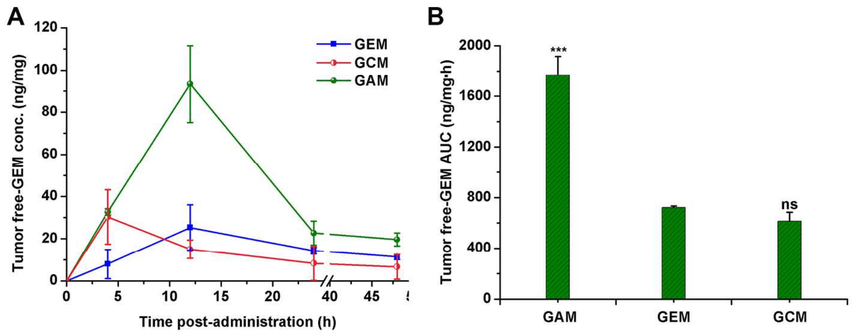

Figure 10. Quantification of tumor free-GEM accumulation for GEM and two prodrugs. (A) Tumor free-GEM concentration-time curves. (B) AUC of free GEM in the tumor, ns: no significance versus GEM, ***P < 0.001 versus GEM (n=3).

To investigate the antitumor efficacy of GAM *in vivo*, 4T1 tumor-bearing mice were randomly divided into four groups and received five injections of vehicle, GEM, GCM and GAM respectively at an equivalent GEM dose of 8 mg/kg per injection. As shown in **Figure 11A**, **11B**, the vehicle group showed a rapid increase in tumor volume (1602 mm^3 at day 22), and GEM was able to somewhat suppress tumor growth but the tumor volume still reached to 595 mm^3 at day 22. In consistent with the *in vivo* tumor free-GEM accumulation result, GCM manifested poor tumor inhibition efficacy, but GAM demonstrated much better antitumor efficacy when compared with GEM. GAM dramatically delayed tumor progression with the final tumor volume of 241 mm^3. The potent antitumor efficacy may be due to: (a) rapid covalently binding of endogenous albumin, (b) good stability in systemic circulation against CDA, (c) long circulation ability, (d) outstanding performance of tumor targeting, (e) independence on hENT, (f) cathepsin B-sensitive GEM release inside tumor cells. All these advantages made GAM a promising candidate for GEM delivery. In addition, GAM demonstrated similar safety profile to GEM confirmed by body weight change (**Figure 11C**), hematological parameters (**Figure 11D**), and H&E stained major organs (**Figure S2**). These suggested that GAM with potent antitumor activity elicited no significant off-target toxicities to major organs.

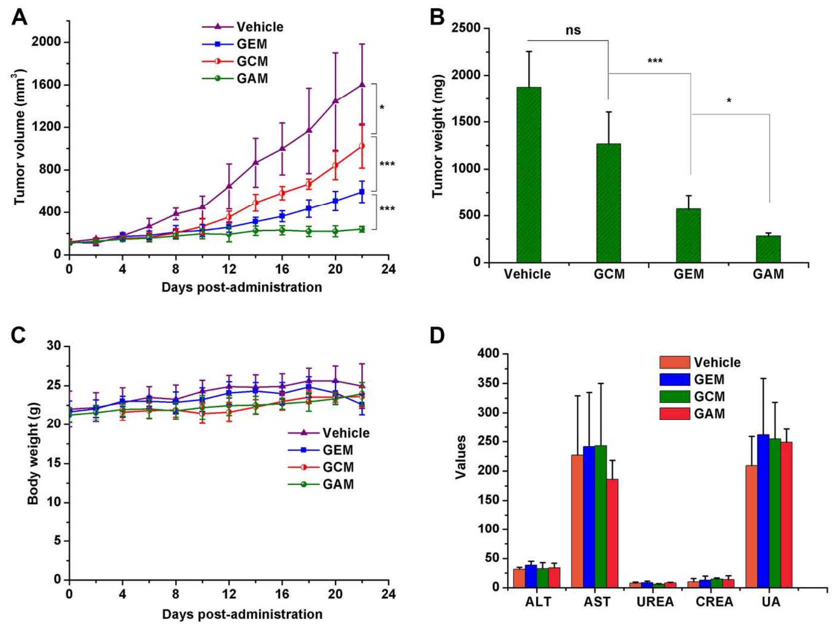

Figure 11. Anticancer efficiency and safety profiles of two prodrugs *in vivo* in a 4T1 tumor xenograft model. (A) Tumor growth curves. (B) Excised tumor weight after last treatment. (C) The weight growth curves of mice, ns: no significance, *P < 0.05, ***P < 0.001 (n=4). (D) Hematological parameters after last treatment (n=3).

In summary, GAM was synthesized for the first time by linking GEM with a maleimide through an amide bond-bearing cathepsin B-sensitive linker. GCM with a carbamate bond-bearing linker was used as a non-enzyme-sensitive control. As a result of covalently targeting circulating albumin and tumor-stimuli-triggered drug release, GAM exhibited distinct superiority over both GEM and GCM in terms of significantly delayed tumor progression and favorable safety profile. The present study successfully exhibited how to exploit endogenous albumin as a carrier to circumvent as many obstacles as possible in GEM delivery through the combination of *in vivo* macromolecular prodrug strategy and ingenious selection of site-specific drug release.

ASSOCIATED CONTENT

Supplementary Information

The supporting information is available free of charge on the ACS Publication website at DOI: 10.1021/acs.bioconjchem.xxxxxxx.

AUTHOR INFORMATION

Corresponding Authors

*E-mail address: hezhonggui@vip.163.com;

*E-mail address: sunjin@syphu.edu.cn.

Notes

The authors declare no competing financial interest.

ACKNOWLEDGMENTS

This work was financially supported by National Natural Science Foundation of China (NO. 81473164, 81573371, 81773656).

REFERENCES

1. Slusarczyk, M., Lopez, M. H., Balzarini, J., Mason, M., Jiang, W. G., Blagden, S., Thompson, E., Ghazaly, E., and McGuigan, C. (2014) Application of ProTide technology to gemcitabine: A successful approach to overcome the key cancer resistance mechanisms leads to a new agent (NUC-1031) in clinical development. *J. Med. Chem. 57*, 1531-1542.

2. Moog, R., Burger, A. M., Brandl, M., Schuler, J., Schubert, R., Unger, C., Fiebig, H. H., and Massing, U. (2002) Change in pharmacokinetic and pharmacodynamic behavior of gemcitabine in human tumor xenografts upon entrapment in vesicular phospholipid gels. *Cancer. Chemoth. Pharm. 49*, 356-366.

3. Damaraju, V. L., Damaraju, S., Young, J. D., Baldwin, S. A., Mackey, J., Sawyer, M. B., and Cass, C. E. (2003) Nucleoside anticancer drugs: the role of nucleoside transporters in resistance to cancer chemotherapy. *Oncogene 22*, 7524-7536.

4. Raetz, C., Chu, M., Srivastava, S., and Turcotte, J. (1977) A phospholipid derivative of cytosine arabinoside and its conversion to phosphatidylinositol by animal tissue. *Science 196*, 303-305.

5. Moysan, E., Bastiat, G., and Benoit, J.-P. (2013) Gemcitabine versus modified gemcitabine: A review of several promising chemical modifications. *Mol. Pharm. 10*, 430-444.

6. Fan, Y., Wang, Q., Lin, G., Shi, Y., Gu, Z., and Ding, T. (2017) Combination of using prodrug-modified cationic liposome nanocomplexes and a potentiating strategy via targeted co-delivery of gemcitabine and docetaxel for CD44-overexpressed triple negative breast cancer therapy. *Acta. Biomater. 62*, 257-272.

7. Wilhelm, S., Tavares, A. J., Dai, Q., Ohta, S., Audet, J., Dvorak, H. F., and Chan, W. C. W. (2016) Analysis of nanoparticle delivery to tumours. *Nat. Rev. Mater. 1*, 16014.

8. Riber, C. F., Zelikin, and A. N. (2017) Recent advances in macromolecular prodrugs. *Curr. Opin. Colloid. In. 31*, 1-9.

9. Soyez, H., Schacht, E., and Vanderkerken, S. (1996) The crucial role of spacer groups in macromolecular prodrug design. *Adv. Drug. Delive. Rev. 21*, 81-106.

10. Kratz, F., Warnecke, A., Scheuermann, K., Stockmar, C., Schwab, J., Lazar, P., Druckes, P., Esser, N., Drevs, J., Rognan, D., et al. (2002) Unger, C. Probing the cysteine-34 position of endogenous serum albumin with thiol-binding doxorubicin derivatives. Improved efficacy of an acid-sensitive doxorubicin derivative with specific albumin-binding properties compared to that of the parent compound. *J. Med. Chem.45*, 5523-5533.

11. Unger, C., Häring, B., Medinger, M., Drevs, J., Steinbild, S., Kratz, F., and Mross, K. (2007) Phase I and pharmacokinetic study of the (6-maleimidocaproyl)hydrazone derivative of doxorubicin. *Clin. Cancer. Res. 13*, 4858-4866.

12. Kratz, F., and Elsadek, B. (2012) Clinical impact of serum proteins on drug delivery. *J. Control. Release. 161*, 429-445.

13. Guo, D.-S., Wang, K., Wang, Y.-X., and Liu, Y. (2012) Cholinesterase-responsive supramolecular vesicle. *J. Am. Chem. Soc. 134*, 10244-10250.

14. Gong, F., Peng, X., Luo, C., Shen, G., Zhao, C., Zou, L., Li, L., Sang, Y., Zhao, Y., and Zhao, X. (2013) Cathepsin B as a potential prognostic and therapeutic marker for human lung squamous cell carcinoma. *Mol. Cancer. 12*, 125.

15. Eiján, A. M., Sandes, E. O., Riveros, M. D., Thompson, S., Pasik, L., Mallagrino, H., Celeste, F., and Casabé, A. R. (2003) High expression of cathepsin B in transitional bladder carcinoma correlates with tumor invasion. *Cancer 98*, 262-268.

16. Gu, M., Wang, X., Toh, T. B., and Chow, E. K.-H. (2017) Applications of stimuli-responsive nanoscale drug delivery systems in translational research. *Drug. Discov. Today.* DOI: 10.1016/j.drudis.2017.11.009.

17. Hacker, S. M., Buntz, A., Zumbusch, A., and Marx, A. (2015) Direct monitoring of nucleotide turnover in human cell extracts and cells by fluorogenic ATP analogs. *ACS. Chem. Biol. 10*, 2544-2552.

18. Lin, T., Zhao, P., Jiang, Y., Tang, Y., Jin, H., Pan, Z., He, H., Yang, V. C., and Huang, Y. (2016) Blood–Brain-Barrier-penetrating albumin nanoparticles for biomimetic drug delivery via albumin-binding protein pathways for antiglioma therapy. *ACS Nano 10*, 9999-10012.

Table of Contents graphic

Maleimide-functionalised cathepsin B-sensitive linker-bearing gemcitabine prodrug dramatically improves pharmacokinetic profiles, tumor cell targeting-bioactivation, and overcomes acquired drug resistance.

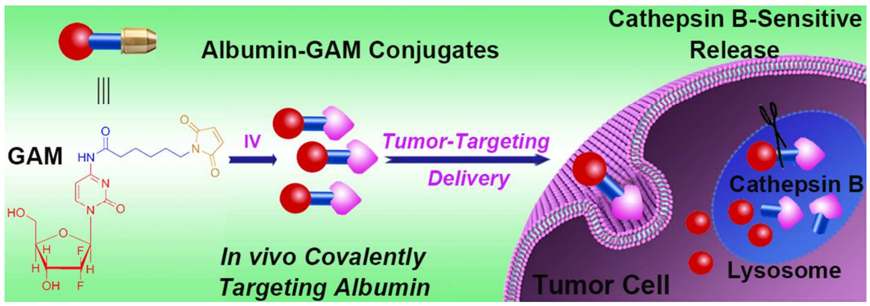

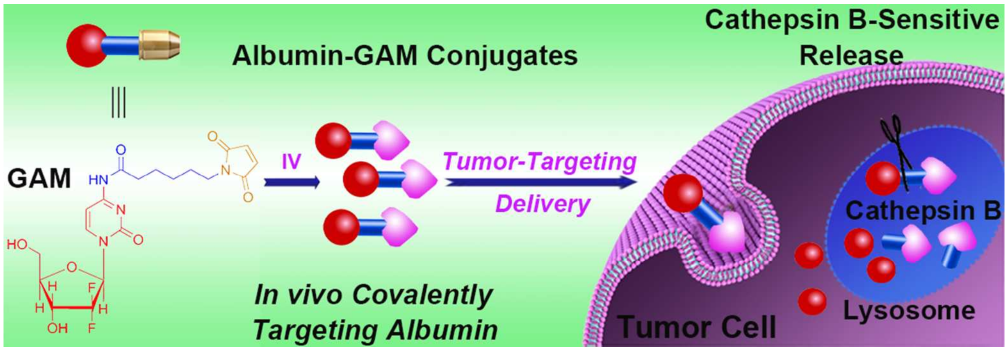

TOC graphic

100x34mm (300 x 300 DPI)

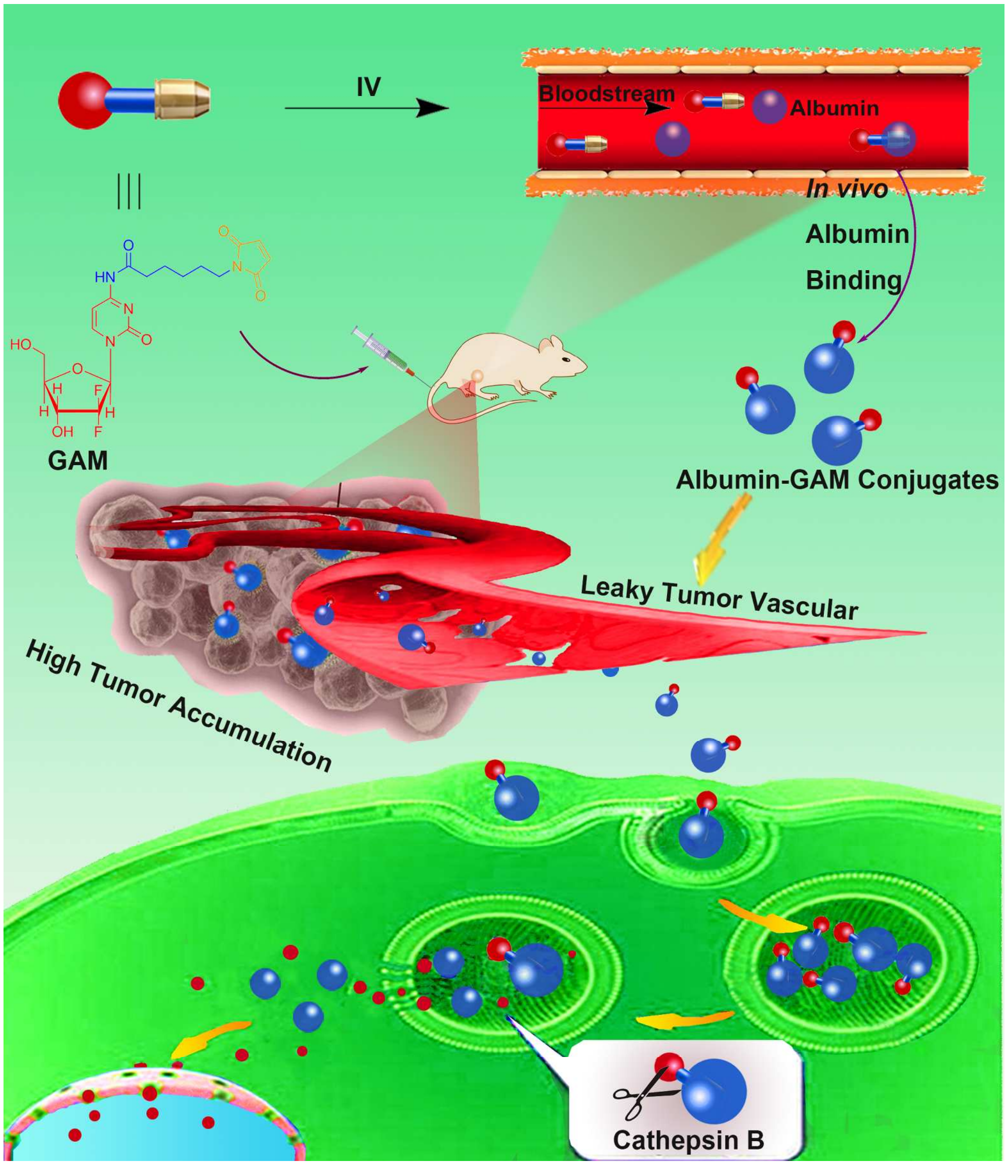

Figure 1. Schematic diagram to describe the whole process of GAM covalently targeting albumin in situ, accumulating at the tumor target and then cathepsin B-mediated parent drug release after intravenous administration.

188x218mm (300 x 300 DPI)

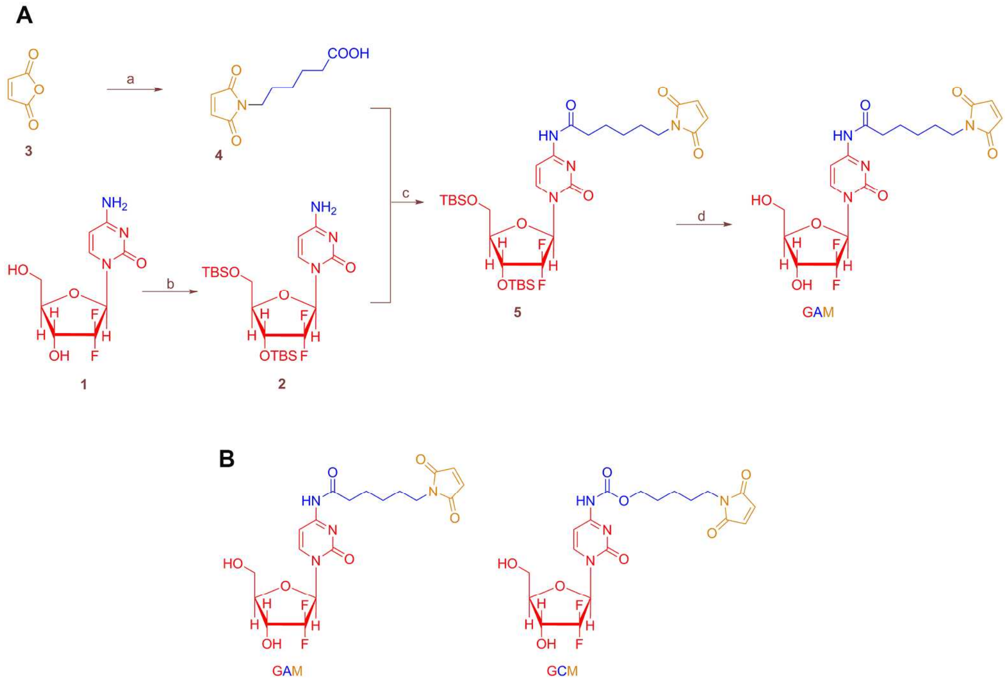

Figure 2. (A) Synthesis of GAM. (B) structures of GAM and GCM.

209x148mm (300 x 300 DPI)

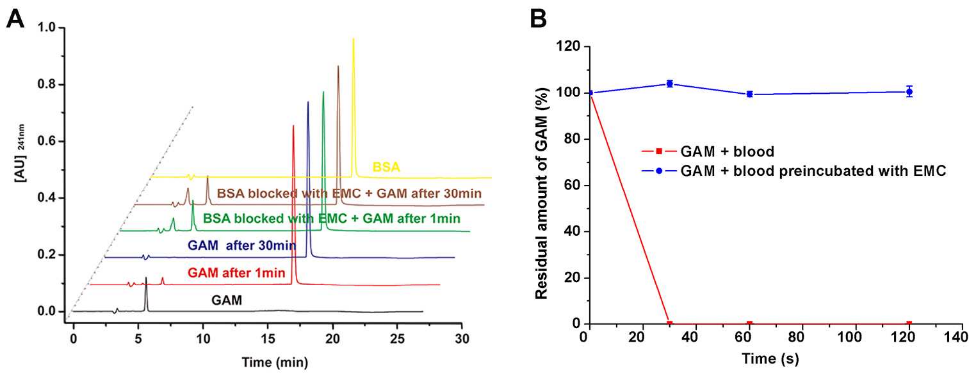

Figure 3. The binding abilities of GAM with albumin at 37°C. (A) Chromatograms. (B) Incubation study of GAM with fresh rat blood (n=3).

190x72mm (300 x 300 DPI)

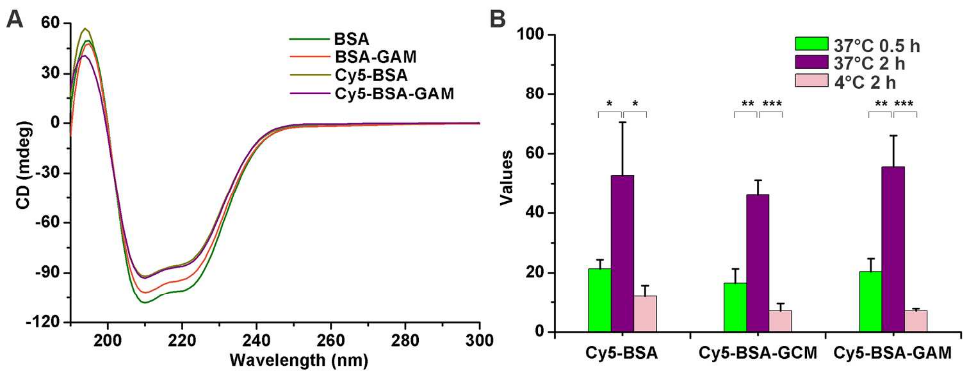

Figure 6. (A) CD spectra of BSA, BSA-GAM, Cy5-BSA and Cy5-BSA-GAM. (B) Cellular uptake of Cy5-BSA, Cy5-BSA-GCM, Cy5-BSA-GAM after incubation with cells at 37°C for 0.5 or 2 h, or at 4°C for 2 h

175x70mm (300 x 300 DPI)

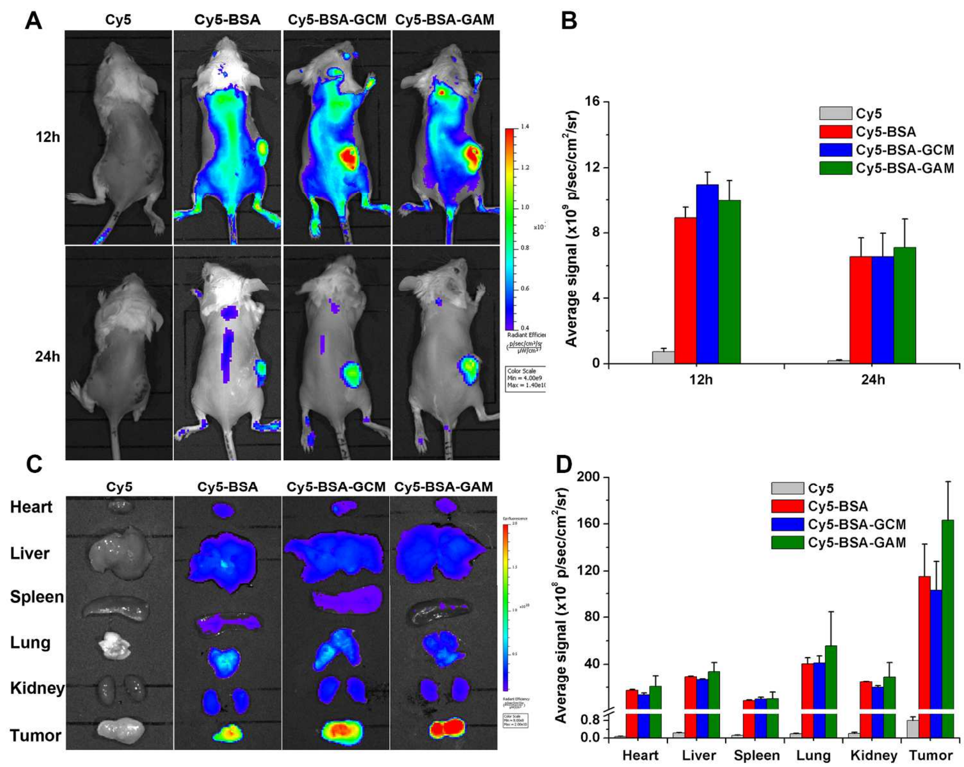

Figure 9. The in vivo and ex vivo fluorescence imaging of 4T1 tumor-bearing mice after intravenously injection of Cy5, Cy5-BSA, Cy5-BSA-GAM and Cy5-BSA-GCM. (A) Whole-body distribution for 12 and 24 h. (B) Quantitative analysis of relative tumor accumulation in a live body. (C) Relative dissected major organs harvested at 24 h post-administration. (D) Quantitative analysis of relative dissected major organs (n=3).

200x156mm (300 x 300 DPI)

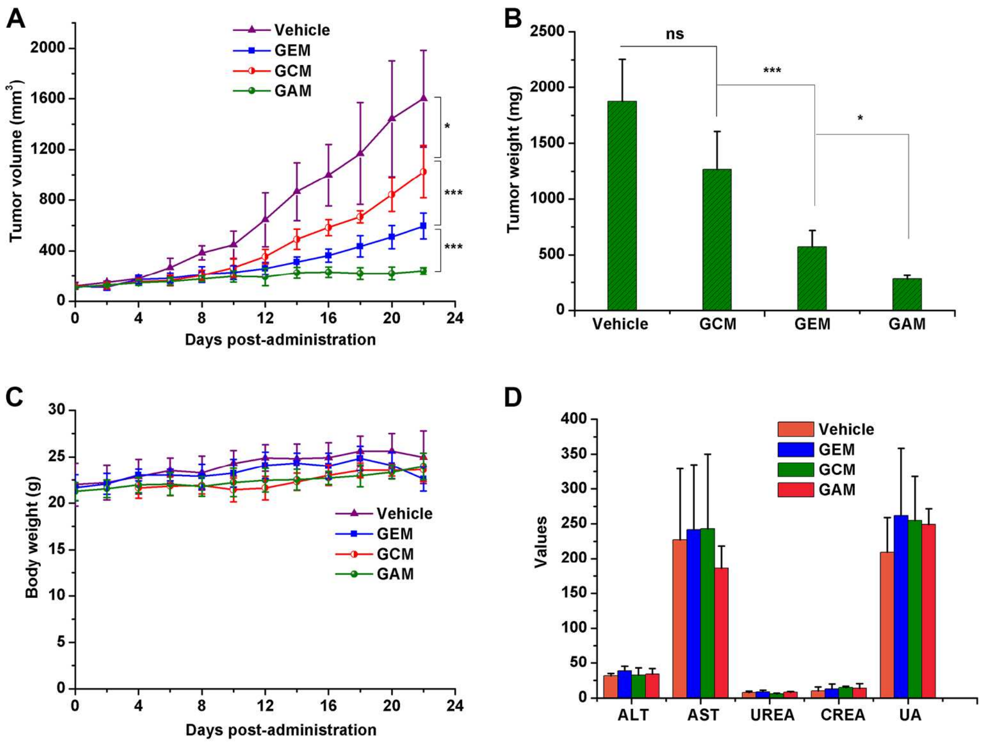

Figure 11. Anticancer efficiency and safety profiles of two prodrugs in vivo in a 4T1 tumor xenograft model. (A) Tumor growth curves. (B) Excised tumor weight after last treatment. (C) The weight growth curves of mice, ns: no significance, *P < 0.05, ***P < 0.001 (n=4). (D) Hematological parameters after last treatment (n=3).

182x139mm (300 x 300 DPI)